Silicon (2020) 12:2837–2850
https://doi.org/10.1007/s12633-020-00380-x

ORIGINAL PAPER

Modified Fractional Photo-Thermoelastic Model for a Rotating Semiconductor Half-Space Subjected to a Magnetic Field

Ahmed E. Abouelregal [1,2]

Received: 26 August 2019 / Accepted: 2 January 2020 / Published online: 28 January 2020

Abstract

The purpose of this work is to introduce a new modified model for photo-thermoelasticity with regard to a new consideration of generalized heat conduction equations with time-fractional order. We consider an isotropic semiconductor half-space which rotating with uniform angular velocity and subjected to a magnetic field. By applying the technique of normal mode analysis, the analytical expressions for the distribution of the displacement components, temperature, carrier density, the thermal stresses, and Lorentz force are obtained and represented graphically. Comparisons are made between the results expected by the modified new fractional model and the classical one. Also, the effects of rotation, the lifetime of the photo-generated, magnetic field and fractional parameter on all the field variables are investigated.

Keywords Thermoelasticity · Time-fractional derivative · Magnetic field · Photothermal · Rotation

1 Introduction

Fractional order differential equations of had been the focal point of many studies because of their common look in numerous applications in viscoelasticity, biology, fluid mechanics, engineering and physics. The most significant improvement by using the usage of differential equations of fractional order in several applications is their nonlocal property. Fractional calculus is a natural extension of classical mathematics. In fact, since the foundation of the differential calculus, the generalization of the concept of derivative and integral to a non-integer order has been the subject of distinct approaches. Due to this reason, there are several definitions [1–3] which are proved to be equivalent. Fractional calculus has been applied in many fields, ranging from statistical physics, chemistry, biological sciences, and economics. In recent years, there has been a great deal of interest in fractional differential equations. Several definitions of the fractional derivative have been proposed. The history and classic transform rules on this subject are well covered in the monograph by Podlubny [4].

During recent years, fractional calculus has also been introduced in the field of thermoelasticity. Povstenko [5] has constructed a quasi-static uncoupled thermoelasticity model based on the heat conduction equation with a fractional-order time derivative. He used the Caputo fractional derivative [6] and obtained the stress components corresponding to the fundamental solution of a Cauchy problem for the fractional-order heat conduction equation in both the one-dimensional and two-dimensional cases. In 2010, a new theory of generalized thermoelasticity in the context of a new consideration of heat conduction with a fractional-order has been proposed by Youssef [7]. In the same year, Sherief et al. [8] have constructed another model in generalized thermoelasticity theory by using fractional time derivatives. Based on the fractional-order thermoelasticity theory, several authors considered thermoelastic problems as given in [9–12].

The classical thermoelastic theory depends on Fourier's law which predicts an unlimited speed of heat propagation. With a specific end goal to wipe out this paradox of infinite speed of thermal propagation, Lord and Shulman [13] introduced a modified thermoelastic theory which is hyperbolic type. The thermoelasticity theory without energy dissipation is a new generalized model introduced by Green and Naghdi [14]. It contains the gradient of thermal-displacement between its independent constitutive variables, and varies from the

✉ Ahmed E. Abouelregal
ahabogal@gmail.com

[1] Department of Mathematics, Faculty of Science, Mansoura University, Mansoura 35516, Egypt

[2] Department of Mathematics, College of Science and Arts, Jouf University, Al-Qurayyat, Saudi Arabia

earlier theories in that it does not accommodate a dissipation of thermal energy.

Investigation of a thermoelastic plane wave in a nonrotating medium is accepting significant attention in later years. Since most huge bodies like the moon, the earth, and different planets have angular velocity, it appears to be more reasonable to discuss the spread of thermoelastic and plane waves in the case of a rotating body. The effect of rotation on heat plane waves is previously considered by several authors [15–19].

Photothermal spectroscopy is a set of great sensitivity methods applied to calculate the thermal characteristics and optical absorption of a specimen. The foundation of photothermal spectroscopy is a photo-generated variation in the condition of the thermal of the specimen. Light energy is absorbed and not missed by subsequent radiation effects in sample heating. This heating causes a change in the temperature as well as changes in the thermodynamic parameters of the sample that are associated with the temperature. Measurements of the pressure, temperature, or density variations caused by the optical absorption are ultimately the basis for the photothermal spectroscopic techniques [20].

There have been various uses of photothermal techniques for material and chemical analysis. Tam [21–23] is maybe first responsible for classifying through the great measure of writing and indicating the purpose of these techniques. A considerable lot of these applications are canvassed in a book proposed by Sell [24]. Spectroscopy is the science offered to the analysis of the interaction of the energy with the matter. The most established orderly technique of the effect of photothermal is accepted to be the correspondence gadget, the photophone, developed by Bell [25, 26]. Bell found that noticeable sound could be heard arriving from the tube fulfilled with different materials when the light shining on the diaphanous tube was modified. The sound was noisy when the tube was fulfilled with radiation assimilating solids or gases, and feeble when loaded with a liquid. The operational standards are currently well understood.

Viengerov [27] used the photoacoustic effect to consider the absorption of light in gases and attained quantitative approximations of concentration in gas blends depend on the signal size. Rosencwaig et al. [28] displayed an examination of the thermoelastic deformations which occur at the surface of the sample due to the excitation by an engaged test beam. Under the generalized thermoelasticity theory, Song et al. [29, 30] presented the bending of semiconducting cantilevers under the thermal optical excitation.

In this work, a new mathematical model of magneto-photo-thermoelasticity has been constructed considering, taking into account a new consideration of heat conduction with non-integer order derivative (fractional derivatives). Based on this model, we have investigated an isotropic semiconductor medium, which is rotated with uniform angular velocity and subjected to a magnetic field. Numerical results of temperature, displacement and stresses are obtained using the normal mode method. Also, the effect of the fractional parameter, magnetic field, rotation and the lifetime of photogenerated on the physical quantities is illustrated graphically and discussed.

2 Basic Equations

Semiconductors are insulator with a dependably little shrouded gaps and shallow vitality levels of electrons bound to polluting influences. The fundamental advantage of a semiconductor is their extraordinary affect ability to debasements: a concentration of impurities like one for each million of host atoms may decide the electrical conductivity and its temperature dependence. The equations of motion of an isotropic magneto-photo-thermoelastic semiconductor material which is rotating with uniform angular velocity $\mathbf{\Omega} = \Omega\mathbf{n}$, ($\mathbf{n}$ the direction of the rotation axis) are given by [31, 32]:

$$(\lambda+\mu)\nabla(\mathrm{div}(\boldsymbol{u}))+\mu\nabla^2\boldsymbol{u}-\gamma\nabla\theta-d_n\nabla N+\boldsymbol{F} \\ =\rho\ddot{\boldsymbol{u}}+\rho\mathbf{\Omega}\times(\mathbf{\Omega}\times\mathbf{u})+\rho\left(2\mathbf{\Omega}\times\dot{\boldsymbol{u}}\right) \tag{1}$$

The absorption of light in a semiconductor causes the optical power to decrease with distance. This effect is described mathematically by the coupled plasma wave equation [28, 29, 33]:

$$D_E\nabla^2N=\rho\frac{\partial N}{\partial t}+\frac{1}{\tau}N+\chi\theta+G \tag{2}$$

The strain-displacement relations are:

$$e_{ij}=\frac{1}{2}\left(u_{i,j}+u_{j,i}\right) \tag{3}$$

The constitutive equations in the photo-thermal medium are:

$$\boldsymbol{\sigma}=\lambda(\mathrm{div}(\boldsymbol{u}))\boldsymbol{I}+\mu\left(\nabla\boldsymbol{u}+\nabla\boldsymbol{u}^{Tr}\right)-(\gamma\theta+d_nN)\boldsymbol{I} \tag{4}$$

During recent years, several interesting models have been developed by using fractional calculus to study the physical processes, especially in the field of heat conduction, diffusion, viscoelasticity, mechanics of solids, control theory, electricity, dielectrics and semiconductors through polymers to fractals, glasses, porous, and random media, porous glasses, polymer chains, and biological systems. It has been realized that the use of fractional order derivatives and integrals leads to the formulation of certain physical problems which is more economical and useful than the classical approach.

There exist many materials and physical situations like amorphous media, colloids, glassy and porous materials, man-made and biological materials/polymers, transient loading, etc., where the classical thermoelasticity based on Fourier type heat conduction breaks down. In such cases, one needs to use a generalized thermoelasticity theory based on an anomalous heat conduction model involving time-fractional (non-integer order) derivatives.

The Riemann-Liouville fractional integral is introduced as a natural generalization of the convolution type integral [34–37]:

$$I^{\alpha} f(t) = \int_0^t \frac{(t-\tau)^{\alpha-1}}{\Gamma(\alpha)} f(\tau) d\tau, \quad \alpha > 0 \tag{5}$$

Where α, $(0 < \alpha < 1)$ is the fractional order parameter, $f(t)$ is a Lebesgue integrable function, $\Gamma(\alpha)$ is the Gamma function and t is the time. In the case that $f(t)$ is absolutely continuous, then

$$\lim_{\alpha \to 1} \frac{d}{d\alpha} f(t) = f'(t) \tag{6}$$

The classical thermoelasticity is based on the principles of the classical theory of heat conductivity, specifically in the traditional Fourier law, which relates the heat flux vector $\boldsymbol{q}$ to the temperature gradient as follows:

$$\boldsymbol{q} = -K \nabla \theta \tag{7}$$

The energy equation is given by

$$\rho C_E \frac{\partial \theta}{\partial t} + \gamma T_0 \frac{\partial}{\partial t} (\mathrm{div}(\boldsymbol{u})) = -\mathrm{div}(\boldsymbol{q}) + \frac{E_g}{\tau} N + Q \tag{8}$$

Equation (7) together with (8) yields a parabolic heat equation. Ezzat [38] constructed a new Fourier model based on the Jumarie Taylor series expansion for fractional-time-derivative [39] given by

$$\left(1 + \frac{\tau_0^{\alpha}}{\alpha!} \frac{\partial^{\alpha}}{\partial t^{\alpha}}\right) \boldsymbol{q} = -K \nabla \theta \tag{9}$$

Taking divergence of both sides of Eq. (7), we get

$$\left(1 + \frac{\tau_0^{\alpha}}{\alpha!} \frac{\partial^{\alpha}}{\partial t^{\alpha}}\right) (\mathrm{div}(\boldsymbol{q})) = -K \nabla^2 \theta \tag{10}$$

From Eqs. (8) and (10), we can get the generalized fractional heat conduction

$$K \nabla^2 \theta = \left(1 + \frac{\tau_0^{\alpha}}{\alpha!} \frac{\partial^{\alpha}}{\partial t^{\alpha}}\right) \left[\rho C_E \frac{\partial \theta}{\partial t} + \gamma T_0 \frac{\partial}{\partial t} (\mathrm{div}(\boldsymbol{u})) - \frac{E_g}{\tau} N - Q\right] \tag{11}$$

In Eqs. (1)–(11), $\boldsymbol{u}$ displacement vector, N is the carrier density, $\theta = T - T_0$ denote the thermodynamic temperature, T_0 is the reference temperature, δ_{ij} is Kronecker's delta, ρ is the mass density, $\boldsymbol{\sigma}$ is the stress tensor and $\boldsymbol{F}$ is the Lorentz force. Also, D_E is the diffusion coefficient, E_g is the semiconductor gap energy, d_n are the difference in deformation potential of the conduction and valence bands, χ is the thermal activation coupling parameter, τ is the lifetime of photogenerated electron–hole pairs, $\gamma = (3\lambda + 2\mu)\alpha_t$ is the volume coefficient of thermal expansion, α_t is the coefficient of linear thermal expansion, λ, μ being Lamés constants, e_{ij} is the strain tensor, $e_{kk} = e$ is the cubical dilatation C_E is the specific heat at constant strain, Q is the heat supplied per unit volume from the external world, K is the thermal conductivity of the solid.

As a result of the application of an initial magnetic field $\boldsymbol{H}$, induced magnetic and electric fields $\boldsymbol{h}$ and $\boldsymbol{E}$. The simplified linear equations of the electrodynamics of a slow-moving medium for a thermally and electrically conducting homogeneous elastic solid are given below (neglecting the charge density)

$$\boldsymbol{J} = \nabla \times \boldsymbol{h} - \varepsilon_0 \frac{\partial \boldsymbol{E}}{\partial t}, \quad \nabla \times \boldsymbol{E} = -\mu_0 \frac{\partial \boldsymbol{h}}{\partial t}, \quad \boldsymbol{E} = -\mu_0 \left(\frac{\partial \boldsymbol{u}}{\partial t} \times \boldsymbol{H}\right), \quad \nabla \cdot \boldsymbol{h} = 0 \tag{12}$$

where ∇ the Hamilton arithmetic operator (nabla), $\boldsymbol{J}$ is the current density μ_0 is the magnetic permeability and ε_0 is the electric permeability.

The Maxwell's stress equation is given by the relation

$$\tau_{ij} = \mu_0 \left[H_i h_j + H_j h_i - H_k h_k \delta_{ij}\right] \tag{13}$$

The Lorentz force $\boldsymbol{F}$ (for a perfect conductor) induced by the magnetic field $\boldsymbol{H}$ is

$$\boldsymbol{F} = \mu_0 (\nabla \times \boldsymbol{H}) \tag{14}$$

3 Statement of the Problem

We consider a semiconductor material to be a homogeneous and isotropic with a rectangular coordinate system (x, y, z). The semiconductor medium is rotating regularly with angular velocity $\boldsymbol{\Omega} = (0, \Omega, 0)$ about the y-axis and under an initial fixed magnetic field $\boldsymbol{H_0}$. Given that the problem is two-dimensional and therefore all functions depend on the spatial variables x and z as well as on the time t. Then the displacement components are

$$\boldsymbol{u} \equiv (u, 0, w) \tag{15}$$

The cubical dilatation given by

$$e = \mathrm{div}(\boldsymbol{u}) = \frac{\partial u}{\partial x} + \frac{\partial w}{\partial z} \tag{16}$$

Using the Maxwell's equation (12), the components of Lorentz force can be expressed as:

$$F_x=\mu_0H_0^2\left(\frac{\partial^2u}{\partial x^2}+\frac{\partial^2w}{\partial x\partial z}-\mu_0\varepsilon_0\frac{\partial^2u}{\partial t^2}\right),\quad F_z=\mu_0H_0^2\left(\frac{\partial^2w}{\partial z^2}+\frac{\partial^2u}{\partial x\partial z}-\mu_0\varepsilon_0\frac{\partial^2w}{\partial t^2}\right)\tag{17}$$

Also, the constitutive equations (4) may be reduced to

$$\begin{aligned}\sigma_{xx}&=(\lambda+2\mu)\frac{\partial u}{\partial x}+\lambda\frac{\partial w}{\partial z}-\gamma\theta-d_nN\\ \sigma_{zz}&=(\lambda+2\mu)\frac{\partial w}{\partial z}+\lambda\frac{\partial u}{\partial x}-\gamma\theta-d_nN\\ \sigma_{xz}&=\mu\left(\frac{\partial u}{\partial z}+\frac{\partial w}{\partial x}\right)\end{aligned}\tag{18}$$

The equations of motion can be obtained by using Eqs. (1), (17) and (18) in the form:

$$\left(\lambda+\mu+\mu_0H_0^2\right)\frac{\partial e}{\partial x}+\mu\nabla^2\mathrm{u}-\gamma\frac{\partial\theta}{\partial x}-d_n\frac{\partial N}{\partial x}=\left(\rho+\varepsilon_0\mu_0^2H_0^2\right)\frac{\partial^2\mathrm{u}}{\partial t^2}-\rho\Omega^2u+2\rho\Omega\frac{\partial w}{\partial t}\tag{19}$$

$$\left(\lambda+\mu+\mu_0H_0^2\right)\frac{\partial e}{\partial z}+\mu\nabla^2\mathrm{w}-\gamma\frac{\partial\theta}{\partial z}-d_n\frac{\partial N}{\partial z}=\left(\rho+\varepsilon_0\mu_0^2H_0^2\right)\frac{\partial^2\mathrm{w}}{\partial t^2}-\rho\Omega^2u-2\rho\Omega\frac{\partial u}{\partial t}\tag{20}$$

The fractional equation of heat conduction (11) can be written as ($Q = 0$)

$$K\left(\frac{\partial^2\theta}{\partial x^2}+\frac{\partial^2\theta}{\partial z^2}\right)=\left(1+\frac{\tau_0^\alpha}{\alpha!}\frac{\partial^\alpha}{\partial t^\alpha}\right)\left[\rho C_E\frac{\partial\theta}{\partial t}+\gamma T_0\frac{\partial e}{\partial t}-\frac{E_g}{\tau}N\right]\tag{21}$$

In addition, the coupled plasma equation (3) in x-z plane will be

$$D_E\left(\frac{\partial^2N}{\partial x^2}+\frac{\partial^2N}{\partial z^2}\right)=\rho\frac{\partial N}{\partial t}+\frac{1}{\tau}N+\chi\theta\tag{22}$$

The displacement vector $\boldsymbol{u}$ can be expressed as

$$\boldsymbol{u}=\nabla\Phi+\mathrm{curl}(\boldsymbol{\Psi})\tag{23}$$

where Φ and $\boldsymbol{\Psi}$ are the displacement potentials which are associated with displacement components u and w as,

$$u=\frac{\partial\Phi}{\partial x}-\frac{\partial\Psi}{\partial z},\qquad w=\frac{\partial\Phi}{\partial z}+\frac{\partial\Psi}{\partial x}\tag{24}$$

Substituting Eq. (24) into Eqs. (19)–(21), we obtain

$$\left(c_0^2\nabla^2+\Omega^2-\left(1+\varepsilon_0\mu_0a_0^2\right)\frac{\partial^2}{\partial t^2}\right)\Phi=\frac{1}{\rho}\left(\gamma\theta+d_nN+2\Omega\frac{\partial\Psi}{\partial t}\right)\tag{25}$$

$$\left(c_3^2\nabla^2+\Omega^2-\left(1+\varepsilon_0\mu_0a_0^2\right)\frac{\partial^2}{\partial t^2}\right)\Psi=2\Omega\frac{\partial\Phi}{\partial t}\tag{26}$$

$$K\left(\frac{\partial^2\theta}{\partial x^2}+\frac{\partial^2\theta}{\partial z^2}\right)=\left(1+\frac{\tau_0^\alpha}{\alpha!}\frac{\partial^\alpha}{\partial t^\alpha}\right)\left[\rho C_E\frac{\partial\theta}{\partial t}+\gamma T_0\frac{\partial}{\partial t}\left(\nabla^2\Phi\right)-\frac{E_g}{\tau}N\right]\tag{27}$$

Where

$$c_0^2=c_1^2+a_0^2,c_3^2=c_2^2+a_0^2,\quad c_1^2=\frac{\lambda+2\mu}{\rho},\quad a_0^2=\frac{\mu_0H_0^2}{\rho},\qquad c_2^2=\frac{\mu}{\rho}.$$

By introducing Eq. (24) into Eq. (18), we get

$$\begin{aligned}\sigma_{xx}&=\lambda\nabla^2\Phi+2\mu\frac{\partial}{\partial x}\left(\frac{\partial\Phi}{\partial x}-\frac{\partial\Psi}{\partial z}\right)-\gamma\theta-d_nN\\ \sigma_{zz}&=\lambda\nabla^2\Phi+2\mu\frac{\partial}{\partial z}\left(\frac{\partial\Psi}{\partial x}+\frac{\partial\Phi}{\partial z}\right)-\gamma\theta-d_nN\\ \sigma_{xz}&=2\mu\frac{\partial^2\Phi}{\partial x\partial z}+\mu\left(\frac{\partial^2\Psi}{\partial x^2}-\frac{\partial^2\Phi}{\partial z^2}\right)\end{aligned}\tag{28}$$

For further attention it is appropriate to introduce the following defined dimensionless quantities:

$$\left\{x',z',u',w'\right\}=\frac{\eta_0}{c_0}\{x,z,u,w\},\quad t'=\eta_0t,\quad\left\{\theta',N'\right\}=\frac{1}{\rho c_0^2}\{\gamma\theta,d_nN\},$$
$$\left\{\Phi',\Psi'\right\}=\frac{\eta_0^2}{c_0^2}\{\Phi,\Psi\},\quad\Omega'=\frac{\Omega}{\eta_0},\quad\sigma'_{ij}=\frac{\sigma_{ij}}{\gamma T_0},\quad\eta_0=\frac{\rho C_Ec_0^2}{K}\tag{29}$$

The basic governing equations after using the non-dimensional forms (29) and suppressing the primes reduce to

$$\left(\nabla^2+\Omega^2-\left(1+\varepsilon_0\mu_0a_0^2\right)\frac{\partial^2}{\partial t^2}\right)\Phi=\theta+N+2\Omega\frac{\partial\Psi}{\partial t}\tag{30}$$

$$\left(c_3^2\nabla^2+c_0^2\Omega^2-c_0^2\left(1+\varepsilon_0\mu_0a_0^2\right)\frac{\partial^2}{\partial t^2}\right)\Psi=2c_0^2\Omega\frac{\partial\Phi}{\partial t}\tag{31}$$

$$\frac{\partial^2\theta}{\partial x^2}+\frac{\partial^2\theta}{\partial z^2}=\left(1+\frac{\tau_0^\alpha}{\alpha!}\frac{\partial^\alpha}{\partial t^\alpha}\right)\left[\frac{\partial\theta}{\partial t}+\varepsilon_1\frac{\partial}{\partial t}\left(\nabla^2\Phi\right)-\varepsilon_2N\right]\tag{32}$$

$$\nabla^2N=g_1\frac{\partial N}{\partial t}+g_2N+g_3\theta\tag{33}$$

$$\sigma_{xx}=\frac{\partial u}{\partial x}+C_{12}\frac{\partial w}{\partial x}-\theta-N$$
$$\sigma_{zz}=\frac{\partial w}{\partial z}+C_{12}\frac{\partial u}{\partial x}-\theta-N \quad (34)$$
$$\sigma_{xz}=C_{13}\left(\frac{\partial u}{\partial z}+\frac{\partial w}{\partial x}\right)$$

where

$$\varepsilon_1=\frac{\gamma^2T_0}{\rho^2c_0^2C_E},\quad \varepsilon_2=\frac{\gamma E_g}{\rho C_E\tau d_n},C_{12}=\frac{\lambda}{\lambda+2\mu},$$
$$C_{13}=\frac{\mu}{\lambda+2\mu},$$
$$g_1=\frac{\rho c_0^2}{D_E\eta_0},\quad g_2=\frac{c_0^2}{D_E\eta_0\tau},\quad g_3=\frac{\kappa d_nc_0^2}{D_E\eta_0^2}.$$

4 Solution of the Problem

The solution of the considered physical quantities can be obtained by applying the normal mode analysis, defined by

$$\{u,w,\theta,\Phi,\Psi,N,\sigma_{ij}\}(x,z,t)$$
$$=\left\{u^*,w^*,\theta^*,\Phi^*,\Psi^*,N^*,\sigma_{ij}^*\right\}(x)\mathrm{e}^{\omega t+iaz} \quad (35)$$

where ω is the (complex) frequency constant, $i=\sqrt{-1}$, a is the wave number in the z direction, and $u^*(x)$, $w^*(x)$, $\theta^*(x)$, $\Phi^*(x)$, $\Psi^*(x)$, $N^*(x)$, and $\sigma_{ij}^*(x)$ are the amplitudes of the field quantities. Using Eq. (35), Eqs. (30)–(33) take the forms

$$\left(D^2-\zeta_1\right)\Phi^*=\zeta_6\Psi^*+\theta^*+N^* \quad (36)$$
$$\left(D^2-\zeta_2\right)\Psi^*=\zeta_5\Phi^* \quad (37)$$
$$\zeta_7\left(D^2-a^2\right)\Phi^*=\left(D^2-\zeta_3\right)\theta^*+\zeta_8N^* \quad (38)$$
$$\left(D^2-\zeta_4\right)N^*=g_3\theta^* \quad (39)$$

where

$$\zeta_1=\omega^2\left(1+\varepsilon_0\mu_0a_0^2\right)+a^2-\Omega^2,\zeta_2=a^2+\frac{c_0^2\omega^2}{c_3^2}\left(1+\varepsilon_0\mu_0a_0^2\right)-\frac{\Omega^2c_0^2}{c_3^2},$$
$$\zeta_3=a^2+\omega\left(1+\frac{\tau_0^\alpha}{\alpha!}\omega^\alpha\right),\zeta_4=a^2+\omega g_1+g_2,\quad \zeta_5=\frac{2\Omega c_0^2\omega}{c_3^2},$$
$$\zeta_6=2\omega\Omega,\zeta_7=\omega\varepsilon_1\left(1+\frac{\tau_0^\alpha}{\alpha!}\omega^\alpha\right),\zeta_8=\varepsilon_1\left(1+\frac{\tau_0^\alpha}{\alpha!}\omega^\alpha\right).$$

Eliminating $\theta^*(x)$, $\Psi^*(x)$ and $N^*(x)$ from Eqs. (36)–(39), one obtains

$$\left(D^8-AD^6+BD^4-CD^2+E\right)\Phi^*(x)=0 \quad (40)$$

with

$$A=\frac{(\zeta_2g_3+\zeta_{14})}{g_3},\quad B=\frac{(\zeta_2\zeta_{14}+\zeta_{15}-\zeta_5\zeta_{12})}{g_3},\quad C=\frac{(\zeta_2\zeta_{15}+\zeta_{16}-\zeta_5\zeta_{12}\zeta_9)}{g_3},E=\frac{(\zeta_2\zeta_{16}-\zeta_5\zeta_{12}\zeta_{10})}{g_3},$$
$$\zeta_{16}=\zeta_1\zeta_{10}g_3+a^2\zeta_{11}\zeta_{13},\zeta_{15}=\zeta_1\zeta_9g_3+\zeta_{11}\zeta_{13}+a^2\zeta_{11}+\zeta_{10}g_3,\zeta_{12}=\zeta_6g_3,$$
$$\zeta_{14}=\zeta_1g_3+\zeta_9g_3,\zeta_{13}=\zeta_4-g_3,\quad \zeta_{11}=\zeta_7g_3,\zeta_{10}=\zeta_8g_3+\zeta_3\zeta_4,\zeta_9=\zeta_3+\zeta_4$$

Equation (40) can be moderated to

$$\left(D^2-k_1^2\right)\left(D^2-k_2^2\right)\left(D^2-k_3^2\right)\left(D^2-k_4^2\right)\Phi^*(x)=0 \quad (41)$$

where k_n^2, $n = 1, 2, 3, 4$ are roots of

$$k^8-Ak^6+Bk^4-Ck^2+E=0 \quad (42)$$

The solution of Eq. (41) when Φ^* is bounded at $x\to\infty$, is obtained as

$$\Phi^*(x)=\textstyle\sum_{n=1}^4C_n(a,\omega)\mathrm{e}^{-k_nx} \quad (43)$$

And in the same way we can get

$$\{N^*,\theta^*,\Psi^*\}(x)=\textstyle\sum_{n=1}^4\left\{C_n',C_n'',C_n'''\right\}(a,\omega)\mathrm{e}^{-k_nx} \quad (44)$$

where C_n', C_n'' and C_n''' are different parameters that are defined as

$$C_n'(a,\omega)=H_nC_n(a,\omega),\quad C_n''(a,\omega)$$
$$=L_nC_n(a,\omega),C_n'''(a,\omega)=M_nC_n(a,\omega),$$

with

$$H_n=\frac{\zeta_{11}\left(k_n^2-a^2\right)}{k_n^4-\zeta_9k_n^2+\zeta_{10}},\quad L_n=\frac{\zeta_{11}H_n\left(k_n^2-\zeta_4\right)}{g_3},\quad M_n$$
$$=\frac{\zeta_5}{\left(k_n^2-\zeta_4\right)}$$

Thus, one obtains

$$\{N^*,\theta^*,\Psi^*\}(x)=\sum_{n=1}^4\{H_n,L_n,M_n\}C_n\mathrm{e}^{-k_nx} \quad (45)$$

By introducing expressions (43) and (45) into Eq. (24) after using (35), we get

$$u^*(x) = -\sum_{n=1}^{4}(k_n + iaM_n)C_n e^{-k_n x}$$
$$w^*(x) = \sum_{n=1}^{4}(ia - k_n M_n)C_n e^{-k_n x} \quad (46)$$

Substituting Eqs. (45) and (46) into Eqs. (34) after using (35), then solution for thermal stresses are given by

$$\sigma_{zz}^*(x) = \sum_{n=1}^{4} R_n C_n e^{-k_n x}$$
$$\sigma_{xz}^*(x) = \sum_{n=1}^{4} Q_n C_n e^{-k_n x} \quad (47)$$

Where

$$R_n = -(k_n^2 - a^2)(2\beta^2 - 1) - 2ia\beta^2 k_n M_n - 2a^2\beta^2 - L_n - H_n,$$
$$Q_n = 2ia\beta^2 k_n + a^2\beta^2 + \beta^2 k_n^2 M_n, \quad \beta^2 = \frac{c_2^2}{c_1^2}.$$

5 Applications

We assume that the half-space is exposed to a normal force on the plane ($x = 0$) which depends on time t and the coordinate x such that $(-\infty < x < \infty)$. The Mechanical boundary conditions on the surface $x = 0$ are

$$\sigma_{zz}(0, z, t) = -P, \quad \sigma_{xz}(0, z, t) = 0. \quad (48)$$

The non-dimensional thermal boundary condition at $x = 0$ is given by

$$\left.\frac{\partial\theta(x, z, t)}{\partial x}\right|_{x=0} + h\theta(0, z, t) = 0. \quad (49)$$

where h is the surface heat transfer coefficient; $h \to 0$ corresponds to thermally insulated boundaries and $h \to \infty$ refers to isothermal boundaries.

The boundary condition for the carrier density can be given below [32, 33]:

$$D_E \left.\frac{\partial N}{\partial x}\right|_{x=0} = s_f N(0, z, t), \quad (50)$$

where s_f is the surface recombination velocity.

Substituting the solutions of σ_{zz}, σ_{xz}, θ and N into the boundary conditions (48)–(50), yields the following equations satisfied by the parameters C_n, ($n = 1, 2, 3, 4$):

$$\sum_{n=1}^{4} R_n C_n = -Pe^{-(\omega t + iaz)} = P_1, \quad (51)$$

$$\sum_{n=1}^{4} Q_n C_n = 0, \quad (52)$$

$$\sum_{n=1}^{4} k_n C_n e^{-k_n x} = 0, \quad (53)$$

$$\sum_{n=1}^{3} G_n C_n = 0, \quad G_n = L_n(D_E k_n + s_f). \quad (54)$$

We can put Eqs. (51)–(54) in the following system equation

$$\begin{Bmatrix} C_1 \\ C_2 \\ C_3 \\ C_4 \end{Bmatrix} = \begin{bmatrix} R_1 & R_2 & R_3 & R_4 \\ Q_1 & Q_2 & Q_3 & Q_4 \\ G_1 & G_2 & G_3 & G_4 \\ k_1H_1 & k_2H_2 & k_3H_3 & k_4H_4 \end{bmatrix}^{-1} \begin{Bmatrix} -P_1 \\ 0 \\ 0 \\ 0 \end{Bmatrix}. \quad (55)$$

After applying the inverse of matrix method, we get the values of the four constants C_j, $j = 1, 2, 3, 4$. Hence, we get the final expressions for the temperature and displacement distributions, in addition the distributions of other physical quantities.

6 Numerical Results

In order to discuss the theoretical results obtained, we now present some numerical results. For the purpose numerical analysis, we consider the value of the relevant parameters for isotropic thermoelastic solid as [40].

$$\lambda = 2.696 \times 10^{10} \text{kg m}^{-1}\text{s}^{-2}, \quad \mu = 1.639 \times 10^{10} \text{kg m}^{-1}\text{s}^{-2}, \quad \rho = 1740 \text{ kg m}^{-3},$$
$$K = 2.510 \text{ W m}^{-1}\text{K}^{-1}, \quad C_E = 1.04 \times 10^3 \text{ J kg K}^{-1}, \quad d_n = -9 \times 10^{-31} \text{ m}^3,$$
$$E_g = 1.11 \text{ eV}, \quad D_E = 2.5 \times 10^{-3} \text{ m}^2 \text{ s}^{-1}, s_f = 2 \text{ m s}^{-1}, \tau = 5 \times 10^{-5} \text{ s}, T_0 = 298K$$

The other magnetic constants are taken as

$$\varepsilon_0 = \frac{10^{-9}}{36\pi} \text{ Fm}^{-1}, \quad \mu_0 = 4\pi \times 10^{-7} \text{ Hm}^{-1}, H_0 = \frac{10^7}{4\pi} \text{ Am}^{-1}.$$

Since ω is complex ($\omega = \omega_0 + i\omega_1$), we can take $\omega_0 = 1$ and $\omega_1 = -1$. Also, the calculations are performed with a small value of time $t = 0.02$ and $h \to 0$. The real part of the temperature distribution θ, components of normal displacement u, tangential displacement w, normal force stress σ_{zz}, tangential stress σ_{xz}, carrier charge density N are taken versus distance x at the plane $z = 1$. The variants of the studied field variables have been displayed in Figs. 1,2,3,4,5,6,7,8,9,10,11,12,13,14,15,16,17,18,19,20,21,22,23-,24. It might have been found that the wave of heat moves forward with a limited velocity in the medium with the

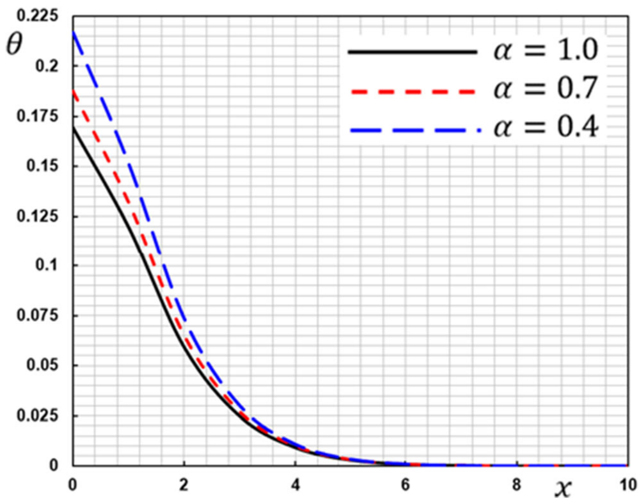

Fig. 1 Variation of temperature θ with distance x for different values of fractional parameter order α

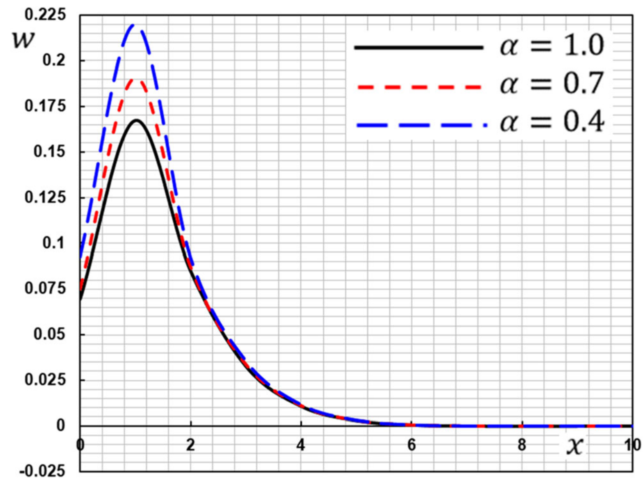

Fig. 3 Variation of displacement w with distance x for different values of fractional order parameter α

passage of time. Comparisons of these non-dimensional physical fields are committed to four different categories.

6.1 Influence of the Fractional Order of Derivative

The present subsection is given over to the display the development of theory of photo-thermoelasticity of a derivative with fractional order and investigates its application to dynamic problems of solid and structural mechanics. The obtained results have been shown, the thermoelastic fractional derivative has been widely applied to generalized thermal problems in solid mechanics.

Figures 1–6 depict the variations of the normal displacement u, tangential displacement w, normal force stress σ_{zz}, tangential stress σ_{xz}, temperature distribution θ and carrier charge density N versus x when $z = 1$, $\tau = 0.002$, the rotation parameter $\Omega = 0.2$ and in the absence and presence of fractional derivative ($0 < \alpha \leq 1$). When $\alpha = 1$ indicates the old situation (normal conductivity) and when $0 < \alpha < 1$ indicates the proposed new theory (weak conductivity). From the graphical representations, it is evident that all curves are coincident when x tends to infinity, all physical fields satisfy boundary conditions. From calculations, we have a significant influence of fractional derivative in the range $0 \leq x \leq 10$. From the figures we found that:

- The distributions of all studied physical quantities tends to zero when the distance x attend to infinity.
- The temperature field starts with positive values and attains its peak values near the surrounding surface, for the three cases ($\alpha = 1$, $\alpha = 0.7$ and $\alpha = 0.4$), which investigates the effect of fractional derivative and show that the particles transfer heat to other particles readily. This

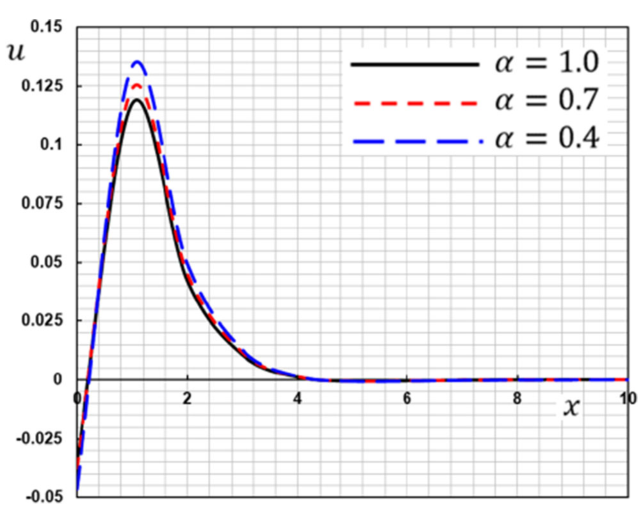

Fig. 2 Variation of displacement u with distance x for different values of fractional order parameter α

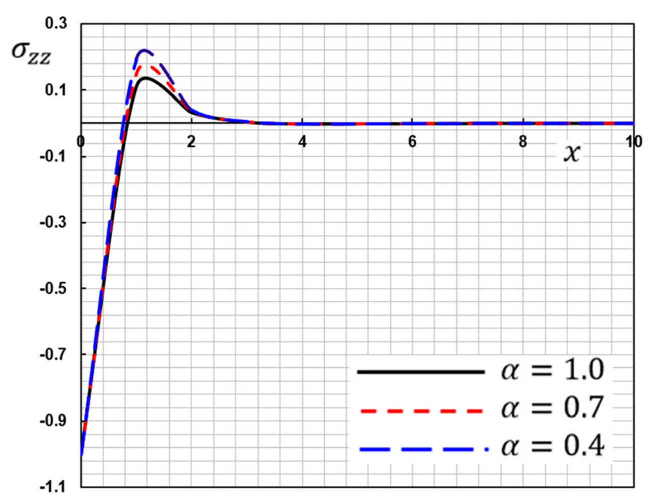

Fig. 4 Variation of the stress σ_{zz} with distance x for different values of fractional order parameter α

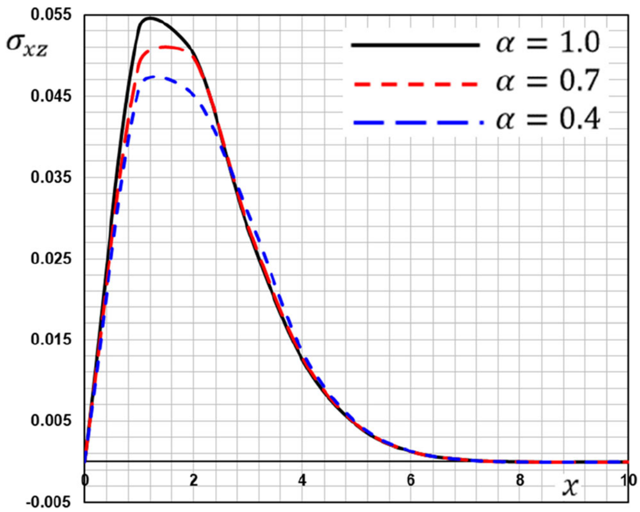

Fig. 5 Variation of the stress σ_{xz} with distance x for different values of fractional order parameter α

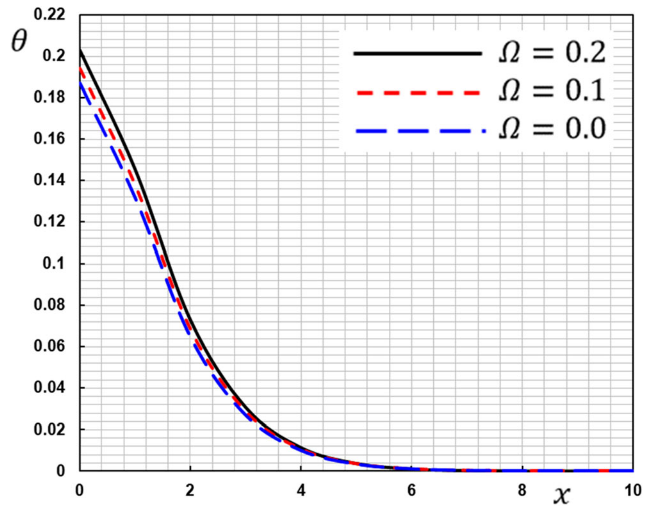

Fig. 7 Variation of temperature θ with distance x for different values of rotation Ω

corresponds to Ezzat's observation in [37]. Also, as x increases, the value of θ decreases to zero value which is quite reasonable (see Fig. 1).

- The fractional derivative has noticeable effects on the profile of the temperature field. However, this field has qualitatively similar behavior for the three cases.
- It is evident that the parameter α acts to decrease the distribution of the temperature field. The time when the temperature reaches the steady-state is approximately the same for each α value.
- As given in the reference [41], it is clear from Fig. 2 that, under the influence of the fractional derivative, the normal displacement u increases with decreasing values of the fractional parameter α.
- The real part of displacement field w starts with values 0.0695263, 0.0749603 and 0.092605 for the three values of the parameter α (1.0, 0.7, and 0.4), which clearly show that that the fractional parameter has a significant effect on the displacement w profile.
- Obviously, as fractional parameter values increase, they having an obligation to decrease pattern of numerical values of displacement w.
- Figure 3 investigates that when the conductivity is normal ($\alpha = 1$), the variation of the magnitude of w profile is the maximum.
- As shown in Fig. 4, the stress component σ_{zz} starts with a negative value and decreases exponentially with the passage of time and then finally decreases to zero as the distance x increases.
- The stress σ_{zz} start with the value $\sigma_{zz} = -P = -1$ at $x = 0$ which verifies that it satisfies the surface condition at the boundary $x = 0$.

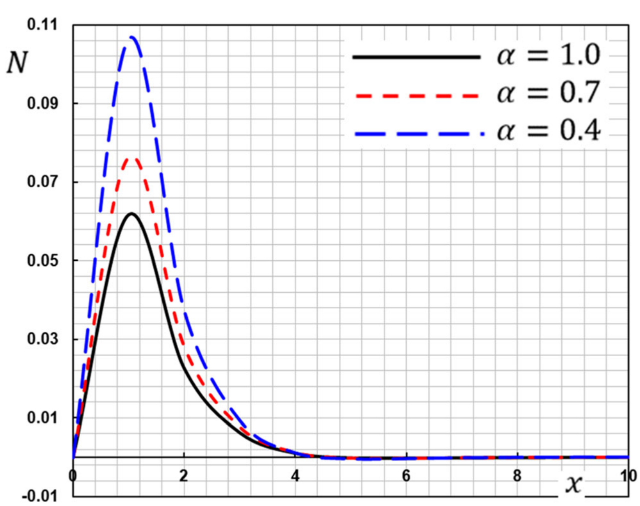

Fig. 6: Variation of carrier density N with distance x for different values of fractional order parameter α

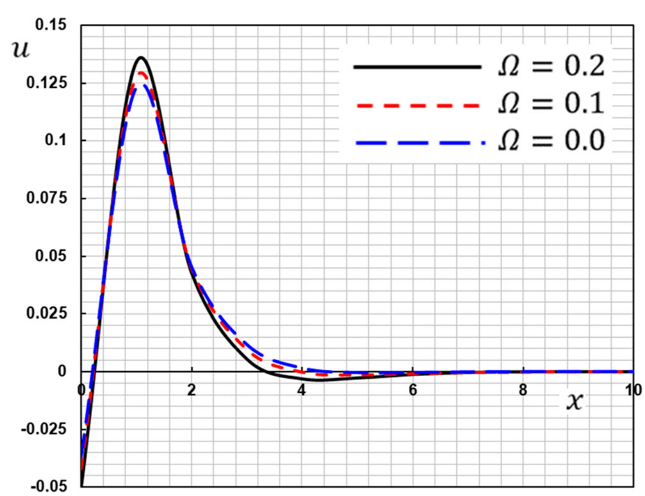

Fig. 8 Variation of displacement u with distance x for different values of rotation Ω

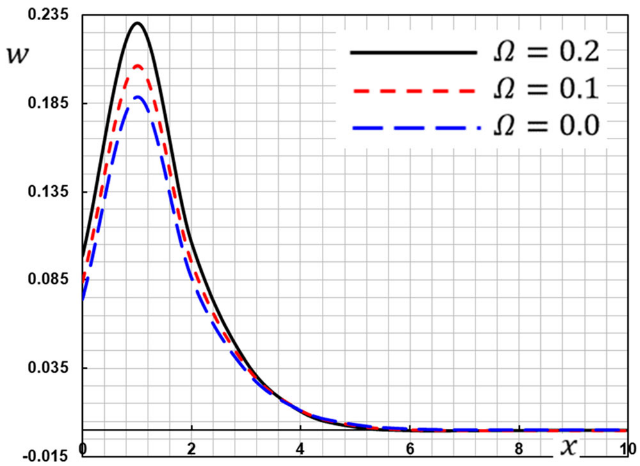

Fig. 9 Variation of displacement w with distance x for different values of rotation Ω

- Figures 4 show that the distribution of stress σ_{zz} is higher when $\alpha = 0.4$ than the values in the case $\alpha = 0.7, 1$ which verify that the fractional parameter has a decreasing effect on field σ_{zz}.
- The variations of the stress σ_{xz} having a common starting point of zero magnitudes which conforms to the surface boundary condition.
- The profile of σ_{xz} is compressive in nature near the plane $x = 0$ and with the increase of x, the stress σ_{xz} decreases to zero value which is quite acceptable.
- The fractional parameter α increases the amplitudes of the stress σ_{zz}.
- The fractional parameter α has a significant effect on carrier density distribution N.
- The carrier density N increases initially and starts to decrease at $x = 1$ (maximum) and finally converges to zero values with x increasing.

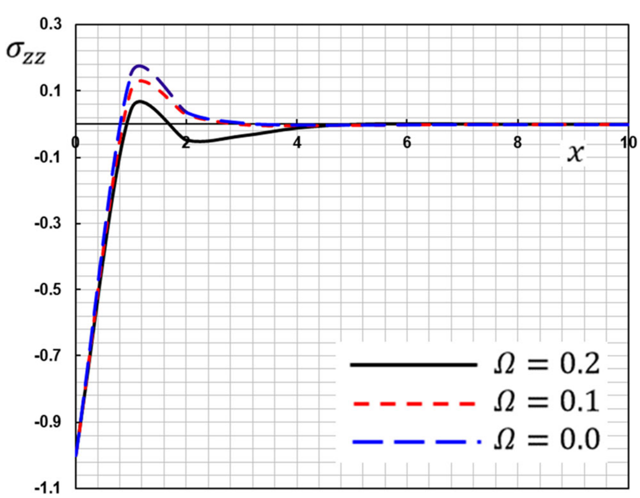

Fig. 10 Variation of stress σ_{zz} with distance x for different values of rotation Ω

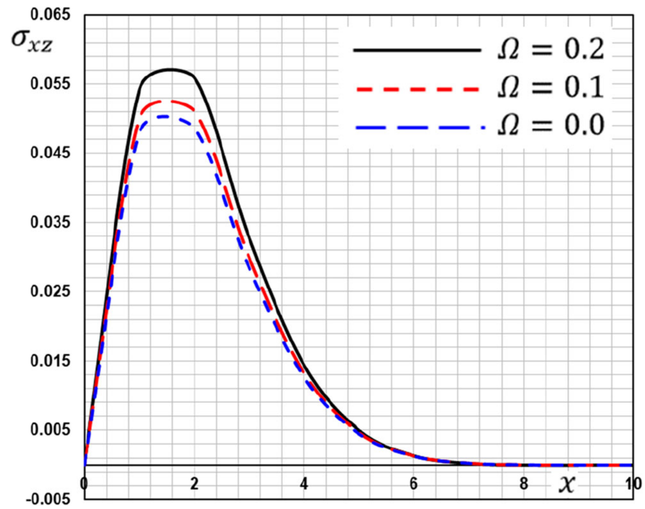

Fig. 11 Variation of stress $\sigma_{xz}$with distance x for different values of rotation Ω

- The phenomenon of limited velocities of the thermal signals in the fractional photo-thermoelasticity theory can be clearly understood by all these figures [12, 42].
- Except for the stress σ_{xz}, all distributions have only non-zero values in a surface area of the body. Outside this region, distributions vanish typically which is in conformity with the experimental results. This demonstrates that the design depends on the hyperbolic heat conduction model is a greater amount physically sensible over that depend on the Fourier law of heat conduction.
- According to our results and the corresponding results in [10, 11, 43], we need to develop a new classification to every one of the materials as per their fractional coefficient, where this parameter turns out to be new pointer of its capacity to conduct the thermal energy.

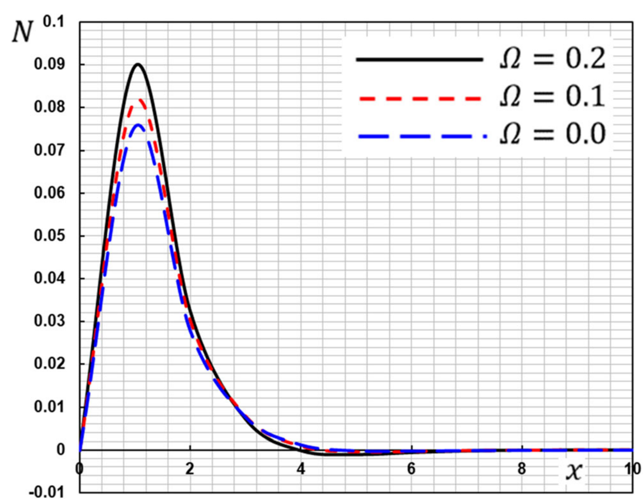

Fig. 12 Variation of carrier charge density N for distance x for different values of rotation Ω

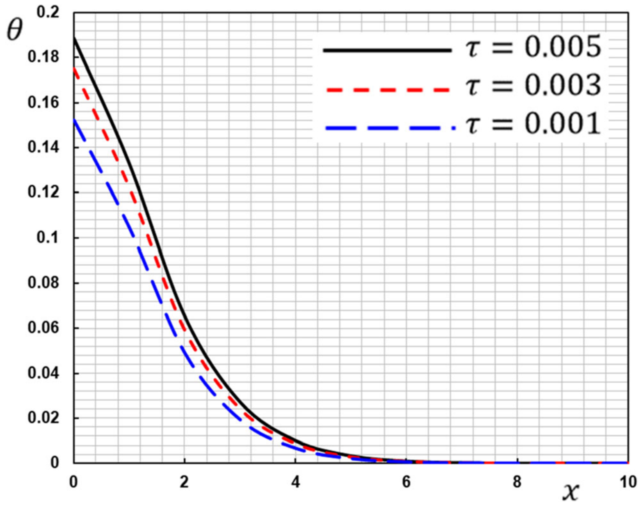

Fig. 13 Variation of temperature θ with distance x for different values of carrier lifetime parameter τ

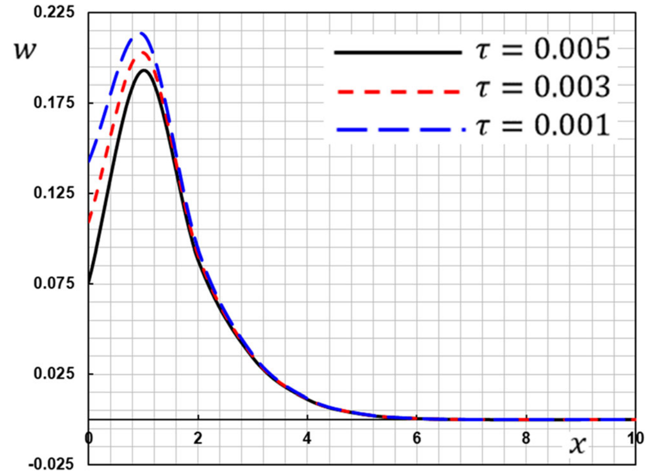

Fig. 15 Variation of displacement w with distance x for different values of carrier lifetime parameter τ

6.2 Influence of the Rotation

When the medium rotates with an angular velocity Ω, we establish the centripetal acceleration and Coriolis increasing speed as two further terms in the equation of motion, affecting the thermoelastic response. In this case, we consider three different values of the rotation parameter Ω = 0, 0.1, 0.2, while the other parameters are taken as $z = 1$, $\tau = 0.002$, and $\alpha = 0.7$. Figures 7-12 are plotted to give a comparison of the results obtained for normal displacement u, tangential displacement w, normal force stress σ_{zz}, tangential stress σ_{xz}, temperature distribution θ and carrier charge density N against positions x in the absence and presence of the angular velocity (rotation parameter) Ω. From all these figures, it is evident that

- All curves coincident when x tends to infinity, all physical fields satisfy boundary conditions.
- The rotating field has noticeable effects on all the profiles of the studied fields.
- The rotation increase the magnitudes of the temperature θ and then decrease their values. This important observation is consistent with the result in [44].
- Also agree with the result in [44], the rotation parameter Ω acts to increase the displacements u, w, the stress σ_{xz} and the carrier charge density field N whereas reducing the normal stress σ_{zz}.
- It is concluded from Figs. 7-12 that all variables depend on time t and space (x, z) as well as the characteristic parameter of the angular velocity Ω. As a result, the study of the displacements and stresses as well as temperature in the presence rotation is very significant in such designs.

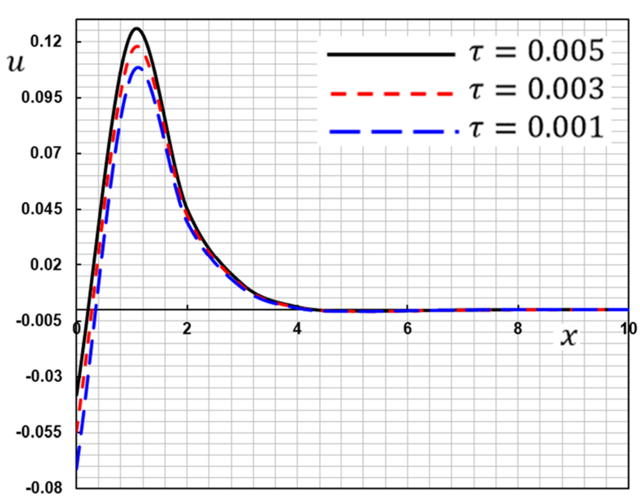

Fig. 14 Variation of displacement u with distance x for different values of carrier lifetime parameter τ

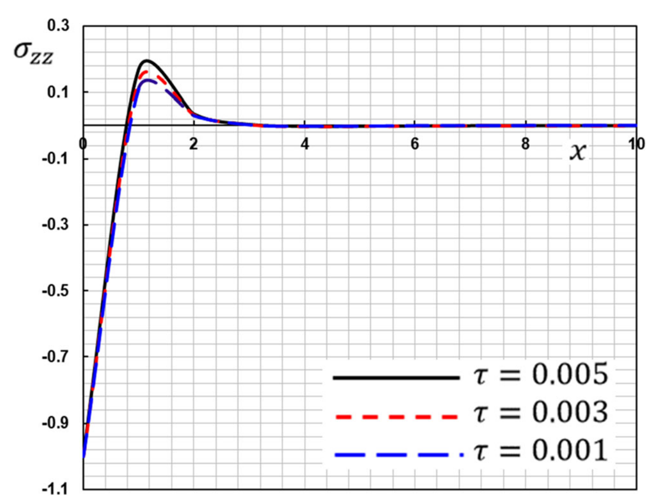

Fig. 16 Variation of stress σ_{zz} with distance x for different of carrier lifetime parameter τ

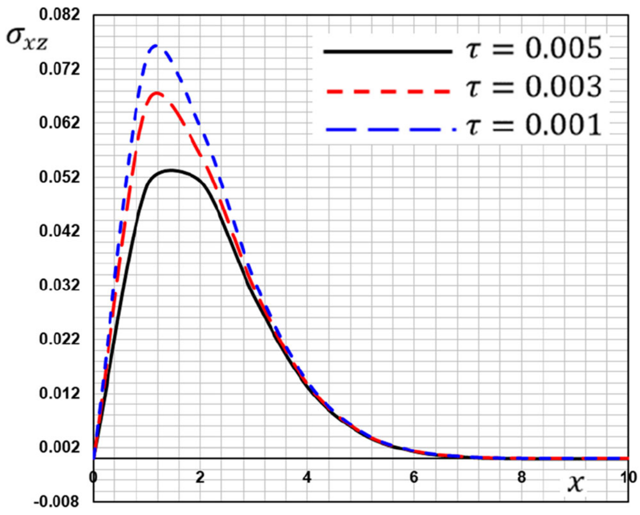

Fig. 17 Variation of stress σ_{xz} with distance x for different values of carrier lifetime parameter τ

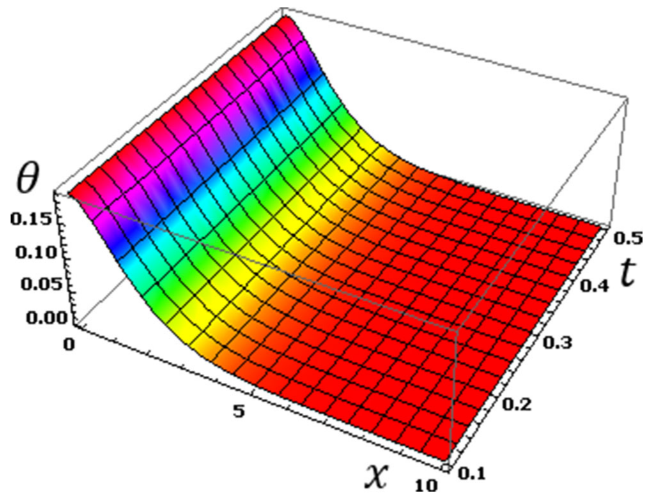

Fig. 19 Variation of temperature θ with distance x for different values of instant time t

6.3 Influence of the Photo-Generated Carrier Lifetime Parameter

The distribution of normal displacement u, tangential displacement w, normal force stress σ_{zz}, tangential stress σ_{xz}, temperature distribution θ and carrier charge density N due to the influence of the photo-generated carrier lifetime parameter τ with distance x are shown in Fig. 13-18. The computations are performed when as $z = 1$, $\Omega = 0.1$, and $\alpha = 0.7$. It is observed that:

- The parameter of carrier lifetime τ has significant effects on all physical fields [45, 46].
- The effect of the carrier lifetime parameter increases the profile of all field variables along the horizontal distance x.

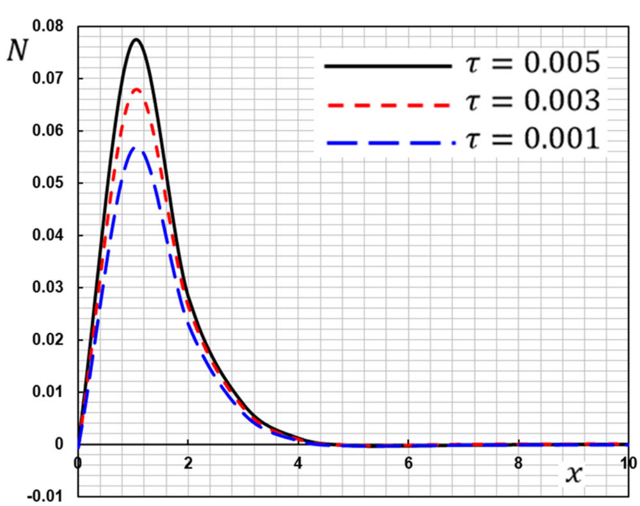

Fig. 18 Variation of carrier charge density N with distance x for different values of carrier lifetime parameter τ

- The phenomenon of limited speeds of heat propagation is emerged in all of these graphs.
- The results achieved, in this case, can be valuable for designers of new materials and other fields in material science and physical engineering to meet special engineering requirements for design of various semiconductor elements, in the presence of the plasma and elastic waves

6.4 Effects of Time Instant on the Studied Field Variables

In the context of the fractional heat conduction model, Figs. 19-24 exhibit the 3D curves for study of the distributions of displacements, temperature change, stress forces and carrier charge density with the change in distance x and instant time t. From the figures, it is noticed that:

- The instant time t has significant effects on all the fields.
- The parameter t plays a vital role in the development of temperature, stresses, carrier charge density and displacements fields.
- The physical fields at in any fixed point (x, z) increase when t increases.
- Figures 17, 18 show that stress components σ_{zz} and σ_{xz} satisfy the boundary condition at $x = 0$ and have a different behavior.
- The comparison of these figures shows the effect of instant time t on the field variable.
- The field quantities including temperature, conductive temperature, displacement components u, w, carrier charge density N and stress components σ_{zz} and σ_{xz} depend not only on spaces x and z, but also on the time t.

Fig. 20 Variation of displacement u with distance$x$ for different values of instant time t

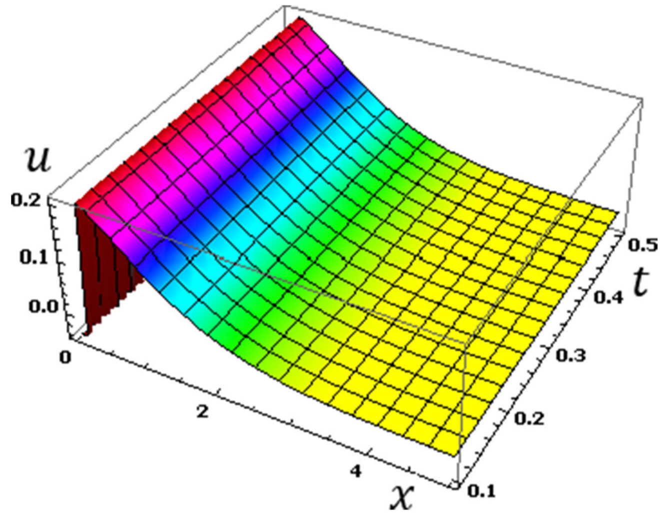

7 Concluding Remarks

In this work, we introduce a new mathematical model of photo-thermoelasticity with fractional order of time derivatives as a new branch of research. In literature, there are only a few numbers of investigations based on our model. Analysis of normal displacement, tangential displacement, normal force stress, tangential stress and temperature distribution due to mechanical load in a generalized thermoelastic semiconductor medium is an interesting problem of mechanics. The following results can be deduced according to the results obtained from our study:

1. The technique used in the current work is suitable for a wide range of problems in photo-thermoelasticity and thermodynamics.
2. The presence of the centripetal acceleration and Coriolis field plays an important role in the physical quantities. The displacements, temperature, and thermal stress of all the physical quantities decrease or increase while the rotating parameter increases. Therefore, studying the existence of the rotation field in this current modified model is of great importance.
3. The presence of photo-thermal field has affected all the considered physical variables. It increases the temperature and the stresses while it reducing the displacements magnitude.
4. The effect of the coefficient of the fractional order of time derivative was observed in all the physical quantities.

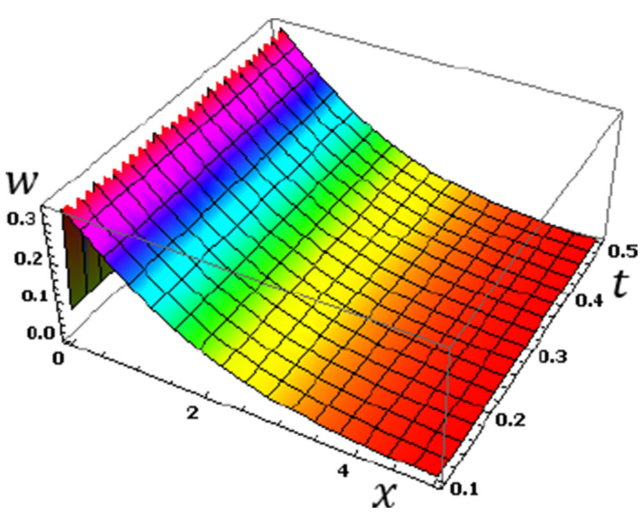

Fig. 21 Variation of displacement w with distance x for different values of instant time t

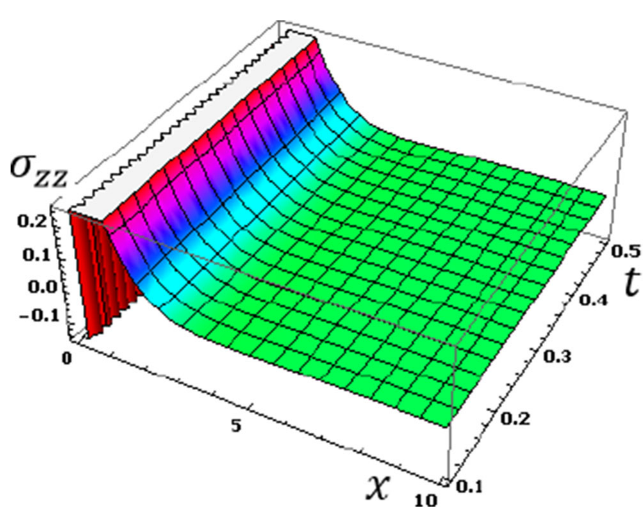

Fig. 22 Variation of stress σ_{zz} with distance x for different values of instant time t

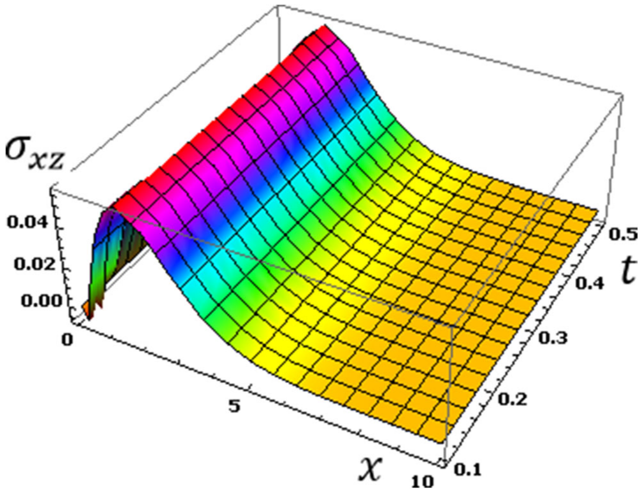

Fig. 23 Variation of stress $\sigma_{xz}$with distance x for different values of instant time t

5. It is seen that the values of all the fields studied are strongly dependent on the carrier lifetime parameter.
6. A significant difference in the values of the studied fields is noticed for different instant time values.
7. All the physical quantities of the body depend on the nature of the applied magnetic field as well as the nature of the boundary conditions
8. This work can useful for investigating and designing materials covered by the thermal, plasma and pulse laser.
9. The results presented in this work will be extremely useful to researchers in terms of physical sciences, material designers, as well as for those working in thermal development and in practical states as in the physics of the earth.
10. Also, this paper suggests that the generalized model of phot- heat transfer of fractional order heat transfer describes the behavior of the thermoelastic body more realistically than the classical theory of phot-thermoelasticity with integer order.

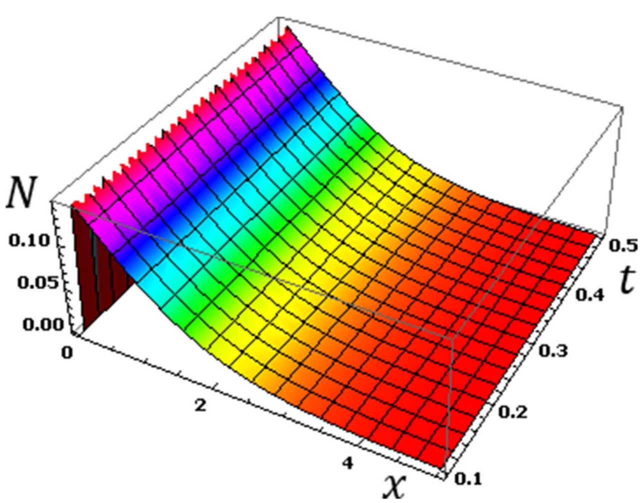

Fig. 24 Variation of carrier charge density N with distance x for different values of instant time t

References

1. Oldham KB, Spanier J (1974) The fractional Calculus: theory and application of differentiation and integration to arbitrary order. Academic Press, New York
2. Samko SG, Kilbas AA, Marichev OI (1993) Fractional integrals and derivatives: theory and applications. Gordon and Breach Science Publishers, London
3. Miller KS, Ross B (1993) An introduction to the fractional Calculus and fractional differential equations. Wiley, New York
4. Podlubny I (1999) Fractional differential equations. Academic Press, New York
5. Povstenko YZ (2005) Fractional heat conduction equation and associated thermal stress. J Therm Stress 28:83–102
6. Caputo M (1967) Linear model of dissipation whose Q is almost frequency independent-II. Geophys J R Astron Soc 13:529–539
7. Youssef H (2010) Theory of fractional order generalized thermoelasticity. J Heat Trans 132:1–7
8. Sherief HH, El-Sayed A, El-Latief A (2010) Fractional order theory of thermoelasticity. Int J Solids Struct 47:269–275
9. Abouelregal AE (2011) Fractional order generalized thermo-piezoelectric semi-infinite medium with temperature-dependent properties subjected to a ramp-type heating. J Therm Stresses 34(11):1139–1155
10. Abouelregal AE, Zenkour AM (2013) The effect of fractional thermoelasticity on a two-dimensional problem of a mode I crack in a rotating fiber-reinforced thermoelastic medium. *Chin. Phys. B* **22**(10):108102 1–8
11. Abouelregal AE (2016) Fractional heat conduction equation for an infinitely generalized, thermoelastic, long solid cylinder. Int J Comput Meth Eng Sci Mech 17(5–6):374–381
12. Zenkour AM, Abouelregal AE (2014) State-space approach for an infinite medium with a spherical cavity based upon two-temperature generalized thermoelasticity theory and fractional heat conduction. Z Angew Math Phys 65(1):149–164
13. Lord H, Shulman Y (1967) A generalized dynamical theory of thermoelasticity. J Mech Phys Solid 15:299–309
14. Green AE, Naghdi PM (1993) Thermoelasticity without energy dissipation. J Elast 31:189–209
15. Sharma JN, Othman MIA (2007) Effect of rotation on generalized thermo-viscoelastic Rayleigh-lamb waves. Int J Solids Struc 44(13):4243–4255
16. Sharma JN, Thakur MD (2006) Effect of rotation on Rayleigh-lamb waves in magneto-thermoelastic media. J Sound Vibr 296(4–5): 871–887
17. Othman MIA, Song YQ (2008) "Reflection of magneto-thermoelastic waves from a rotating elastic half–space", *Int.* J Eng Science 46(5):459–474
18. Othman MIA, Zidan MEM, Hilal M, M.I. (2013) Influence of gravitational field and rotation on Thermoelastic solid with voids under Green-Naghdi theory. J Phys 2:22–34
19. Abouelregal, A.E. and Abo-Dahab, S.M. (2018), "A two-dimensional problem of a mode-I crack in a rotating fibre-reinforced isotropic thermoelastic medium under dual-phase-lag model," *Sadhana*, **43**(1), article no. 13
20. Dovichi, N. J. (1987), "CRC critical reviews in analytical chemistry" **17**, 357

21. Tam AC (1983) *Ultrasensitive Laser Spectroscopy Kliger, D. S.* Academic Press, New York
22. Tam AC (1985) Pulsed photothermal radiometry for noncontact spectroscopy, material testing and inspection measurements. Infrared Physics 25(1):305–313
23. Tam AC (1986) Applications of photoacoustic sensing techniques. Reviews Mod. Phys 58:381–431
24. Sell JA (1989) Photothermal investigations in solids and fluids. Academic Press, Inc, New York
25. Bell AG (1880) On the production and reproduction of sound by light. Am J Sci, Series 3(20):305–324
26. Bell AG (1881) Upon the production of sound by radiant energy. Philos Mag Series 5 11(71):510–528
27. Viengerov ML (1938). Dokl Akad Nauk SSSR 19:687
28. Rosencwaig A, Opsal J, Willenborg DL (1983) Thin-film thickness measurements with thermal waves. Appl Phys Lett 43(2):166–168
29. Song Y, Todorovic DM, Cretin B, Vairac P (2010) Study on the generalized thermoelastic vibration of the optically excited semiconducting microcantilevers. Int J Solids Struct 47(14):1871–1875
30. Song Y, Todorovic DM, Cretin B, Vairac P, Xu J, Bai J (2014) Bending of semiconducting cantilevers under photothermal excitation. Int J Thermophys 35(2):305–319
31. Roychoudhuri SK, Mukhopadhyay S (2000) Effect of rotation and relaxation times on plane waves in generalized thermo-visco-elasticity. Int J Math Math Sci 23:497–505
32. Song YQ, Bai JT, Ren ZY (2012) Study on the reflection of photothermal waves in a semiconducting medium under generalized thermoelastic theory. Acta Mech 223:1545–1557
33. Todorovic DM (2003) Plasma, thermal, and elastic waves in semiconductors. Rev Sci Instrum 74:582
34. Povstenko YZ (2005) Fractional heat conduction equation and associated thermal stress. J. Therm. Stress. 28:83–102
35. Povstenko YZ (2009) Thermoelasticity that uses fractional heat conduction equation. J Math Sci 162(2):296–305
36. Miller KS, Ross B (1993) An introduction to the fractional integrals and derivatives, theory and applications. John Wiley and Sons Inc., New York
37. Podlubny I (1999) Fractional differential equations. Academic press, New York
38. Ezzat MA (2011) Magneto-thermoelasticity with thermoelectric properties and fractional derivative heat transfer. Phys. B 406:30–35
39. Jumarie G (2010) Derivation and solutions of some fractional black-Scholes equations in coarse-grained space and time. Application to Merton's optimal portfolio. Comput Math Appl 59:1142–1164
40. Dhaliwal RS, Singh A (1980) Dynamical coupled thermoelasticity. Hindustan Publishers, Delhi
41. Zenkour AM, Abouelregal AE (2019) Fractional thermoelasticity model of a 2d problem of mode-i crack in a fibre-reinforced thermal environment. J Appl Comput Mech 5(2):269–280
42. Kothari S, Mukhopadhayay S (2011) A problem on elastic half space under fractional order theory of thermoelasticity. J Therm Stress 34:724–739
43. Ezzat MA, Fayik MA (2013) Modeling for fractional ultralaser two-step thermoelasticity with thermal relaxation. Arch Appl Mech 83:1679–1679
44. Said SM, Elmaklizi YD, Othman MIA (2017) A two-temperature rotating-micropolar thermoelastic medium under influence of magnetic field. *Chaos Solit. Fractals* 97:75–83
45. Abbas IA, Aly K (2017) A generalized model on plasma, thermal and elastic waves in a semiconductor medium. *J. Adv. Phys.* **6**(3): 317–325
46. Lotfy K (2017) Photothermal waves for two temperature with a semiconducting medium under using a dual-phase-lag model and hydrostatic initial stress. *Waves Rand. Comp Media* 27(3):482–501